

## **AN ANNUAL CYCLE OF SANDBAR MIGRATION ON AN INTERMEDIATE MESOTIDAL BEACH: ENSENADA, MEXICO.**

Jesús Adrian Vidal-Ruíz <sup>1</sup>, Amaia Ruiz de Alegría-Arzaburu

### **Abstract**

Cross-shore sandbar migration has been studied on a single-barred beach based on monthly measured bathymetric surveys from August 2014 to August 2016. A continuous time-series of nearshore wave measurements allowed the correlation of the onshore and offshore sandbar movement to the incoming wave conditions. The sandbar formed near the shoreline by October 2014, and built up and moved offshore during the 2014–2015 winter from November to February, as a result of the subaerial beach erosion. During that winter the sandbar crest migrated 150–200 m offshore reaching an average depth of 2–2.5 m. The sandbar moved onshore after February 2015, merging the inner intertidal beach by May; from March to April the sandbar and berm coexisted. The beach was unbarred during the 2015 summer waves from June to September, and a berm was built along the upper intertidal beach. The sandbar formed again by October 2015 and migrated 190–250 m offshore during the 2015–2016 El Niño winter, reaching depths of 3–3.5 m. Despite the onshore movement of the sandbar from February to April 2016, it was unable of welding the intertidal beach, thus, the beach was barred from June to August 2016. This study highlights the presence of a strong seasonal sandbar migration cycle in Ensenada Beach, which was interrupted during the 2015–2016 El Niño winter.

**Key words:** beach, morphodynamics, sediment transport, erosion, accretion, El Niño.

### **1. Introduction**

Sandbars are subaerial features usually located in water depths of less than 10 m, across and just seaward of the surf zone. Sandbars play an important role in the morphodynamics of sandy beaches, since they comprise large amounts of sediment and can dissipate up to 80% of the incident wave energy; consequently acting as a natural defense against shoreline erosion and flooding (Walstra, 2016; Yuhi et al., 2016). These features may have a profound impact on the nearshore hydrodynamics depending on their geometry and cross-shore location (Ruessink and Ranasinghe, 2014; Walstra, 2016). The offshore sandbar migrations are generally associated to strong mean offshore currents (undertow) occurring under breaking large wave conditions, while the onshore movement takes place during weak-to-nonbreaking waves and is primarily related to near-bed wave skewness (e.g. Plant et al., 2001; Ruessink et al., 2007; Cohn et al., 2014), wave asymmetry (Plant et al., 2001; Hoefel and Elgar, 2003) and/or boundary layer streaming and Stokes drift (Henderson et al., 2004; Aagaard et al., 2013). The net onshore sandbar migration results from the gradual sediment transport towards the beachface during calm wave periods, and episodic strong offshore sediment transport during high-energy wave conditions cause the net offshore migration (Ojeda et al., 2011; Sénéchal et al., 2015; Walstra, 2016).

Most of the sandbar studies have been focused on multi-barred beaches, and single-barred beaches have been surprisingly understudied (e.g. van de Lageweg et al., 2013; Blossier et al., 2016). The most comprehensive studies on sandbar dynamics were undertaken over decades along the multi-barred beaches of Duck (USA), Terschelling and the Holland Coast (The Netherlands) and Wanganui (New Zealand) (e.g. Lippmann et al., 1993; Ruessink and Kroon, 1994; Shand et al., 1999; Plant et al., 1999). These beaches however, lacked of seasonal sandbar movements and presented interannual migration cycles of bar generation near the shoreline, offshore migration across the surf zone and final stage of sandbar disappearance at the outer nearshore zone (Ruessink and Kroon, 1994).

---

<sup>1</sup> Institute of Oceanographic Research, University of Baja California, Km 103 Tijuana-Ensenada Road, 22860, Ensenada, México. [avidal@uabc.edu.mx](mailto:avidal@uabc.edu.mx); [amaia@uabc.edu.mx](mailto:amaia@uabc.edu.mx)

Despite all these studies, the seasonal sandbar migration is still poorly understood given the expense and difficulties of collecting *in-situ* measurements of sandbars (Di Leonardo and Ruggiero, 2015). These studies require long-term bathymetric measurements of high spatio-temporal resolution to be able to accurately determine the sandbar shape and cross-shore position (e.g. Grunnet and Hoekstra, 2004; Di Leonardo and Ruggiero, 2015), and enable the understanding their spatial variability in response to the storm-driven or seasonal wave forcing (Pape et al., 2010).

## 2. Field site

The study site comprises the northern 3 km of Ensenada beach, located in the northwestern coast of the Baja California peninsula, within Todos Santos Bay (TSB) (Figure 1). The beach is partly protected from the western Pacific swell by Todos Santos Islands (17 km offshore). Ensenada is a single-barred and intermediate beach, made of siliceous medium sand ( $D_{50}$  of 0.25 mm) and with an average slope of  $\tan \beta$  of 0.025 (Ruiz de Alegria-Arzaburu et al., 2015). The beach is mesotidal, and the tides are semi-diurnal with spring to neap tidal ranges of 2.3 m and 0.5 m (<http://oceanografia.cicese.mx/predmar>). The bathymetry within TSB is fairly shallow (depths of up to 50 m) but a deep canyon of over 400 m is present between Todos Santos Islands and the Punta Banda headland.

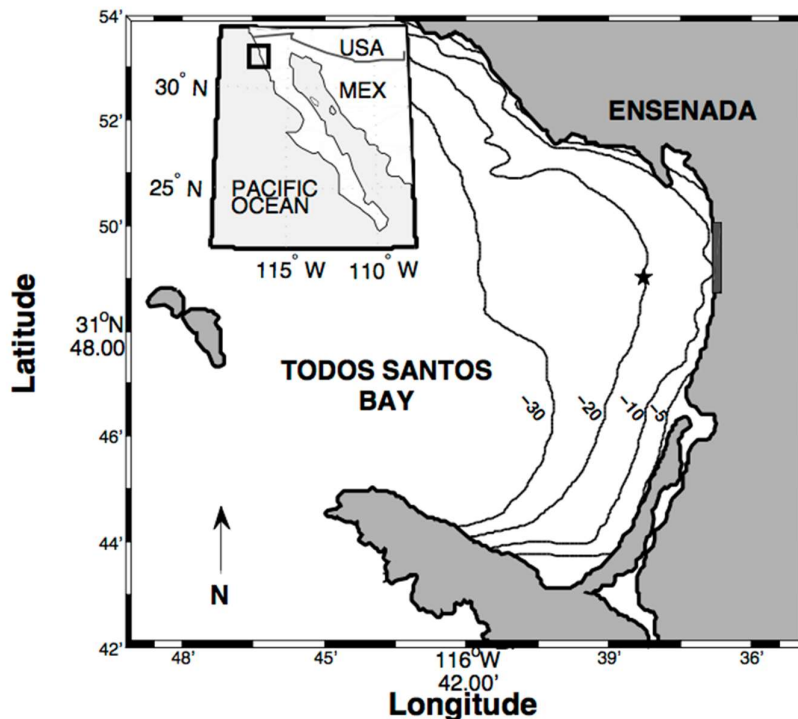


Figure 1. Location of Ensenada Beach (grey longshore rectangle) within Todos Santos Bay, and the northwestern Baja California peninsula in Mexico. The position of the acoustic Doppler profiler (AWAC) at 20 m depth is indicated with a grey star.

Coastal structures exist along the beach, such as a promenade in the northern section and a seawall and rip-rap in the middle section (Figure 2). The southern beach preserves a natural dune backed by a shallow and intermittently dry freshwater lagoon. The walled subaerial beach is 80–120 m wide, whereas the non-walled section has a subaerial width of 220–240 m (Ruiz de Alegria-Arzaburu et al., 2015). The supratidal beach fronting the promenade is up to 6.5 m above mean low water (MLW) and up to 3.5 m on rip-rap and seawall protected sections, while the dunes have a maximum elevation of 10 m above MLW (Figure 2).



Figure 2. View on the study area: (a) beach with a promenade in the northern section, (b) seawall and rip-rap in the middle section, (c) natural dune backed by a freshwater lagoon in the southern section, and (d) southern limit of the study area.

The beach is exposed to the north Pacific and south Pacific swell waves during the winter and summer, respectively. The annual nearshore waves have a mean significant wave height ( $H_s$ ) of 1 m and an average period of 11 s. The mean winter  $H_s$  is 1.5 m (from December to February) with an associated period of 12.5 s. The summer waves (June to August) have an average  $H_s$  of 0.7 m with a shorter wave period of 8 s. Significant wave heights above 4 m represent less than 2% of the annual waves and occur mainly during fall and winter seasons.

### 3. Methods

Morphological measurements were monthly collected over a 2 years period (August 2014 to August 2016) across the subaerial and subtidal sections of nearly 3 km of beach length. The sandbar crest positions were determined and related to the incoming wave forcing.

#### 3.1. Wave measurements

Hourly nearshore wave data were collected from August 2014 to August 2016 with a 1MHz ADCP (Nortek AWAC) located 2.5 km off the beach at a water depth of 20 m (Figure 1). The instrument was installed on the seabed and provided continuous measurements of wave parameters including the significant wave height ( $H_s$ ), wave peak period ( $T_p$ ) and wave direction ( $\alpha$ ). The monthly averaged wave heights were calculated for the years 2014, 2015 and 2016.

#### 3.2. Topographic and bathymetric measurements

The subaerial beach morphology (topography) was measured monthly from August 2014 to December 2016 along a beach section of 2,867 m measuring a total of ~50 m spaced 61 cross-shore profiles during low spring tides. The profiles were measured using a differential GPS (Global Positioning System) with a precision of  $\pm 0.03$  m, and a threshold elevation value of 0.05 m was established to discard post-processed erroneous data as established in other research studies (e.g. Coco et al., 2014). All profiles were measured down to the mean low tide level (MLT) at a frequency of 1Hz using a two-wheeled trolley operated by two people on foot. The measurements were referred in Universal Transverse Mercator (Easting and Northing coordinates in meters), and the elevations were referenced to the local MLT (+36.135 m from ellipsoidal heights). The same transect lines were followed at each survey, as these were mapped on the GPS controller.

The subtidal morphology (bathymetry) was monthly measured from August 2014 to December 2016, right after or before the topographic measurements. The bathymetric data were acquired using the Sontek M9 Hydrosurveyor Acoustic Doppler Current Profiler (ADCP) synchronized to the differential GPS and fixed to a small boat or to a jetski. The frequency of 0.5 MHz was used to obtain the bathymetric data with a sound speed corrected depth accuracy of  $\pm 0.02$  m. Similar to Wijnberg et al. (1995), an accuracy of  $\pm 0.1$  m was estimated when ship-dependent errors were included. In all surveys an overlap with a few topographic lines was obtained, and it was used to verify the adjustment of the submerged elevations to the subaerial. A full survey consisted of 100 m spaced 30 cross-sectional topographic-and-bathymetric profiles (TB), (Figure 3) and comprised depths ranging from 1 to 12 m, beyond the depth of closure ( $\sim 8$  m).

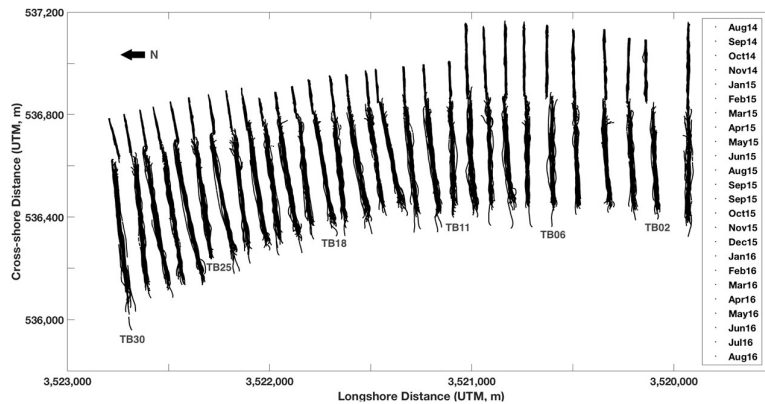


Figure 3. Plan view of the topographic and bathymetric profiles (TB) from August 2014 to August 2016. The cross-shore and longshore distances are in Universal Transverse Mercator (UTM, m).

### 3.3. Sandbar extraction

The sandbar crest positions were extracted from each of the monthly measured TB profiles. The sandbar crests were defined as the positions of maximum vertical differences relative to the August 2014 unbarred profile (circle in Figure 4). The cross-shore sandbar position was determined as the cross-shore distance between the bar crest and the reference shoreline ( $x_C - x_S$ ), and the depths were calculated as the vertical differences from the crest to the reference shoreline ( $z_C - z_S$ ).

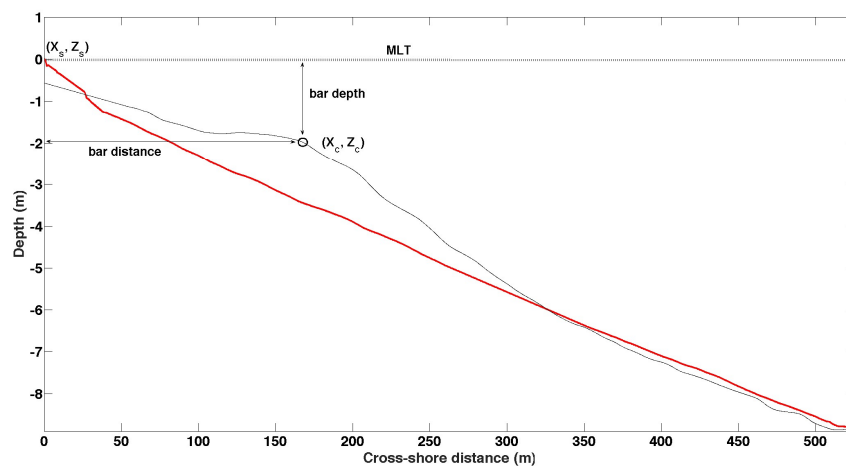


Figure 4. Sandbar crest location (black circle,  $x_C, z_C$ ) for a typical profile (black profile) relative to the August 2014 unbarred profile (red profile) (modified from Di Leonardo and Ruggiero, 2015). The profile elevations are referred to the mean low tide level (MLT).

## 4. Results

### 4.1. Wave conditions

Significant seasonal and interannual differences were encountered in the wave conditions between the years 2014, 2015 and 2016 (Figure 5). The waves were significantly more energetic during the 2015–2016 winter than during the previous winters in 2014 and 2015. The average  $H_s$  exceeded 1.5 m from December 2015 to March 2016 and the waves were of longer period (sometimes over 20 s) during some of the energetic events than in the previous winters.

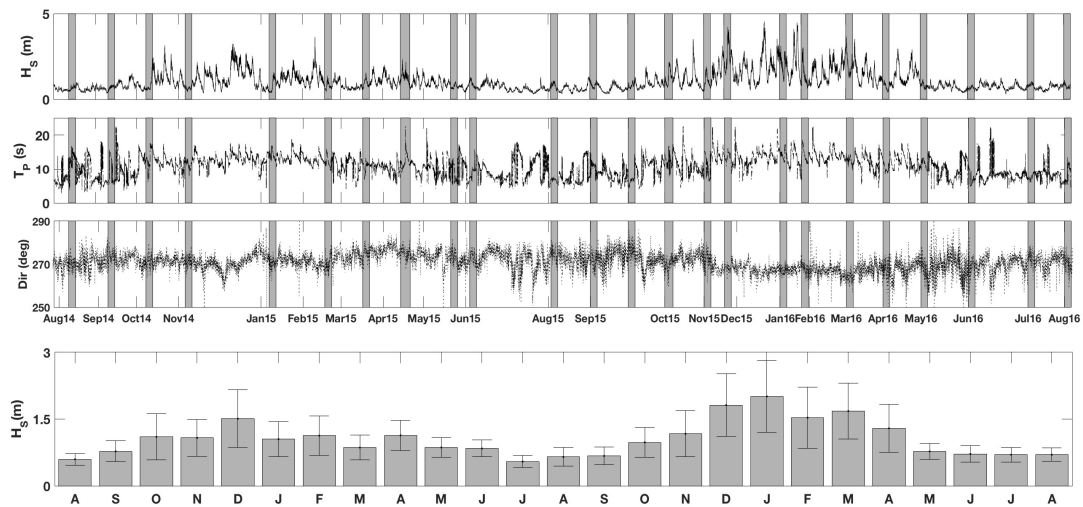


Figure 5. Time series of significant wave height ( $H_s$ ), peak period ( $T_p$ ), wave direction ( $Dir$ ) (top three panels) and monthly averaged  $H_s$  from August 2014 to August 2016 and their standard deviations (bottom panel). The vertical gray bars indicate the times when the morphological measurements (topography and bathymetry) were undertaken.

### 4.2. Beach profile evolution

The topographic-and-bathymetric profile (TB) evolution was studied over a two-year period from August 2014 to August 2016 (Figures 6, 7 and 8) and related to the incident wave conditions. TB 02, 18 and 30 were selected as being the most representative for the southern, middle and northern beach sections. The summer profiles represented by August show an unbarred profile and subaerial beach recovery in 2014 and 2015 with the presence of a berm. In August 2016, however, the subaerial beach does not show a full recovery, and a sandbar is observed at 2.5 m depth, mostly at the southern and middle beach sections (red and cyan profiles in Figures 6, 7 and 8).

In November the beach presents an inner sandbar in co-existence with a berm. The sandbar is located further offshore in the southern and middle beach section (1 to 2 m depth) than in the northern beach end (0.2 m depth), (black profiles in Figures 6, 7 and 8). The sandbar is fully developed and located further offshore by February (blue profiles in Figures 6, 7 and 8) and associated to subaerial beach erosion. The sandbar moved to deeper water in the southern and middle beach sections (3 and 2 m, respectively; Figures 6 and 7) than in the northern section (1.5–2 m, Figure 8), and mostly by February 2016, after El Niño winter.

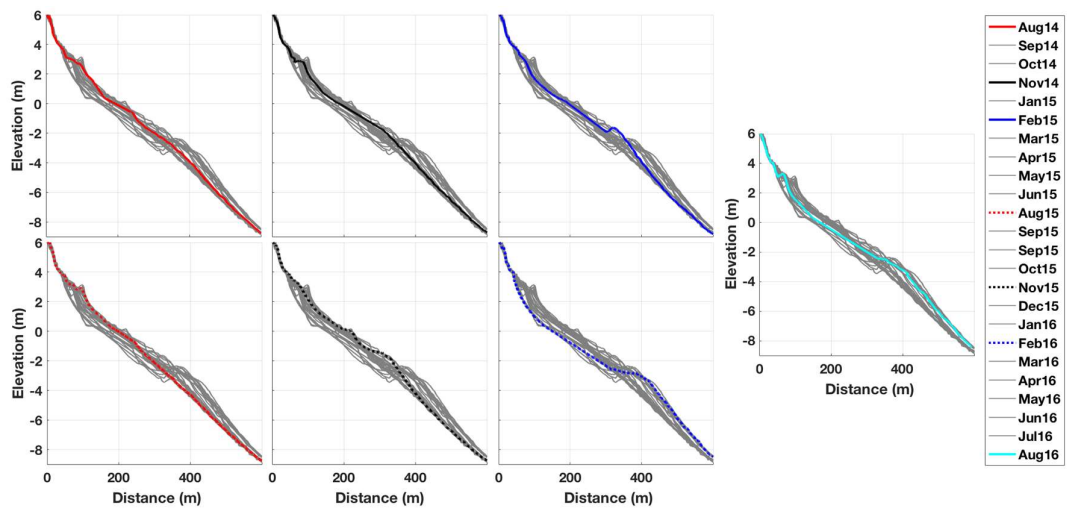


Figure 6. Temporal evolution of TB02 (southern beach) from August 2014 to August 2016 (gray profiles). The August, November and February profiles are highlighted in red, black and blue, respectively. The August 2016 profile is highlighted in cyan.

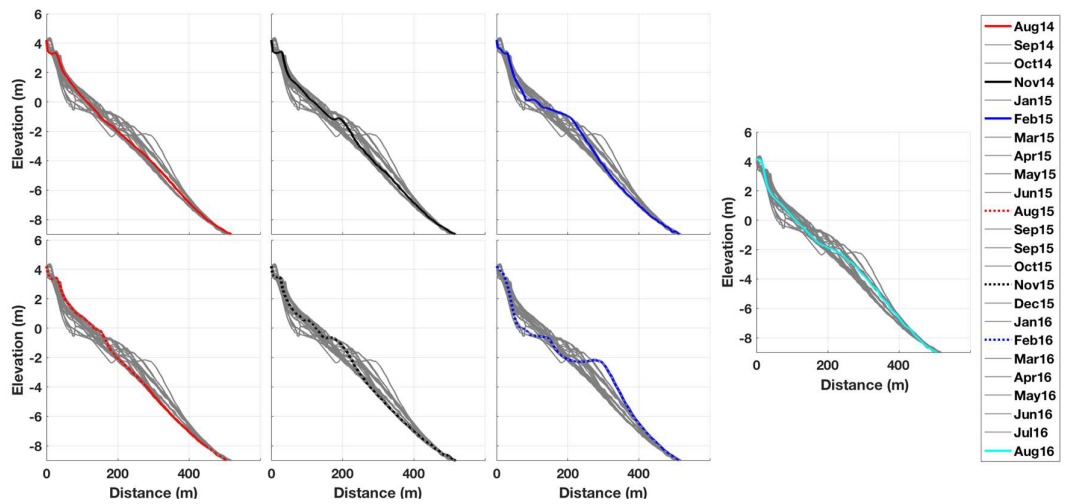


Figure 7. Temporal evolution of TB18 (middle beach) from August 2014 to August 2016 (gray profiles). The August, November and February profiles are highlighted in red, black and blue, respectively. The August 2016 profile is highlighted in cyan.

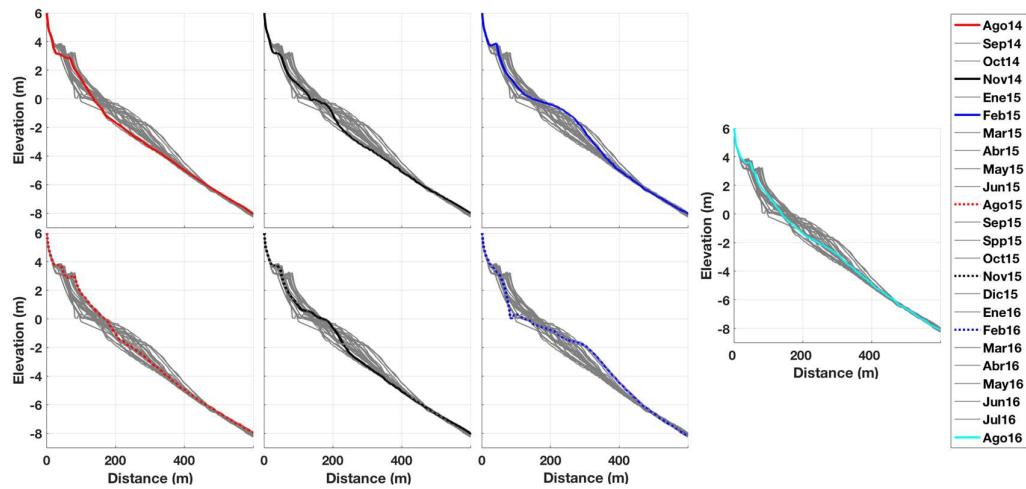


Figure 8. Temporal evolution of TB30 (northern beach) from August 2014 to August 2016 (gray profiles). The August, November and February profiles are highlighted in red, black and blue, respectively. The August 2016 profile is highlighted in cyan.

#### 4.3. Sandbar migration

The sandbar crest positions were obtained for the 02, 06, 11, 18, 25 and 30 TB profiles in order to determine the cross-shore sandbar migration in relation to the different wave conditions (Figures 9, 10 and 11). In 2014 and 2015, the sandbar was formed near the shoreline in September and reached 0.5 to 1 m depth at a distance of 50 to 100 m from the shore by October. Then it migrated 140–190 m offshore between October and February reaching a depth of 2 m, and back onshore between February and April, and being the profile unbarred between May and September (Figures 9, 10 and 11).

The largest offshore migration occurred during 2015–2016 El Niño winter, reaching displacements of 190–200 m from the reference shoreline and maximum depths of 3–3.5 m, mostly in the southern half of the beach (Figures 9, 10 and 11). After the winter, from February to May, the sandbar moved 50–60 m onshore in the southern end (Figure 9) and 80–120 m onshore in the middle and northern ends (Figures 10 and 11). The sandbar maintained in the same cross-shore position between April and July 2016 in the southern end profiles (TB02 and TB06, Figure 9) while the sandbar in the northern end moved further offshore between May and August 2016. The beach maintained barred during the summer period from June to August 2016.

### 5. Discussion

In accordance with previous findings along the southern Pacific US coast indicating the presence of unusually energetic waves related to the El Niño climatic anomaly (Allan and Komar, 2002; Storlazzi and Griggs, 2000; Adams et al., 2008), in Todos Santos Bay the 2015–2016 El Niño winter was characterized by the presence of more energetic waves that lasted for a month or two longer than in previous years. The average significant wave height exceeded 1.5 m from December 2015 to March 2016 and the waves were of longer period (sometimes over 20 s) during some of the energetic events than in the previous winters in 2014 and 2015.

After the energetic 2015–2016 El Niño winter, the sandbar migrated further offshore (190–250 m) than in the previous winters (150–200 m), and reached a depth of 3–3.5 m compared to 2–2.5 m. These findings agree with Ruggiero et al., (2009) in that energetic incident waves generate strong offshore-directed cross-shore mean flows that induce sandbars to migrate further offshore. Moreover, the sandbars did not weld the shore during the 2016 summer, possibly as a consequence of longer energetic winter (till April) that impeded onshore migration due to the lack of long enough fair weather conditions (Ruggiero et al., 2016).

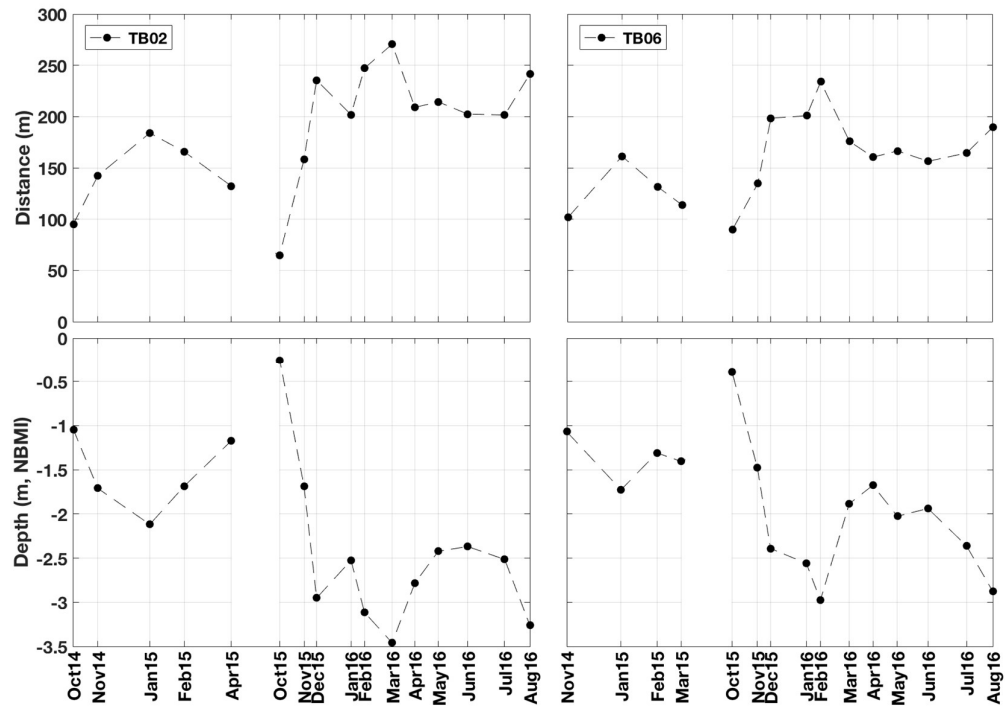


Figure 9. Cross-shore sandbar crest migrations (top panels) at TB02 and TB06 (southern beach) and their associated depths (bottom panels) from October 2014 to August 2016.

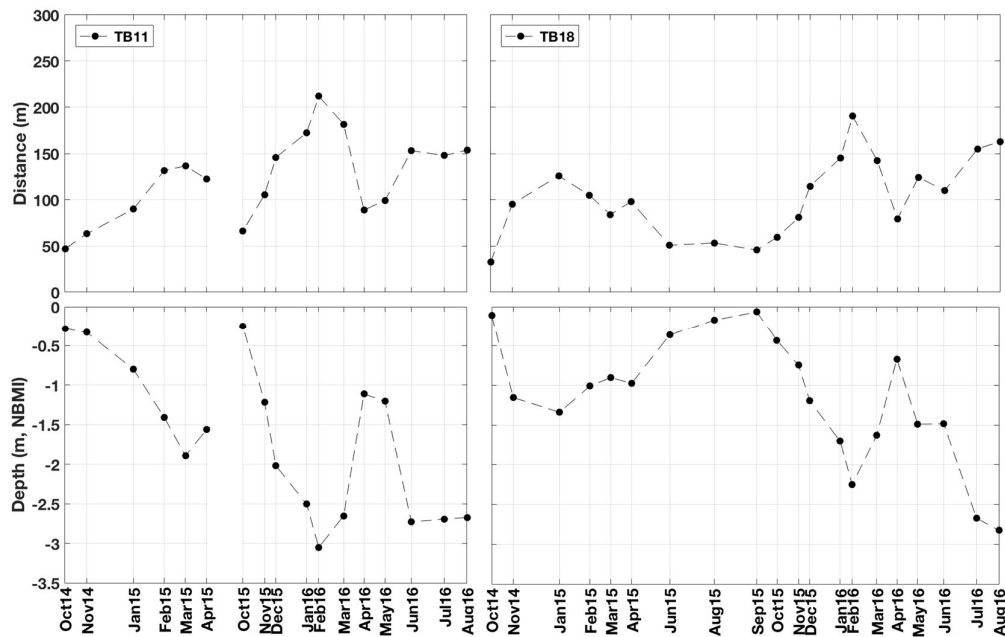


Figure 10. Cross-shore sandbar crest migrations (top panels) at TB11 and TB18 (middle beach) and their associated depths (bottom panels) from October 2014 to August 2016.



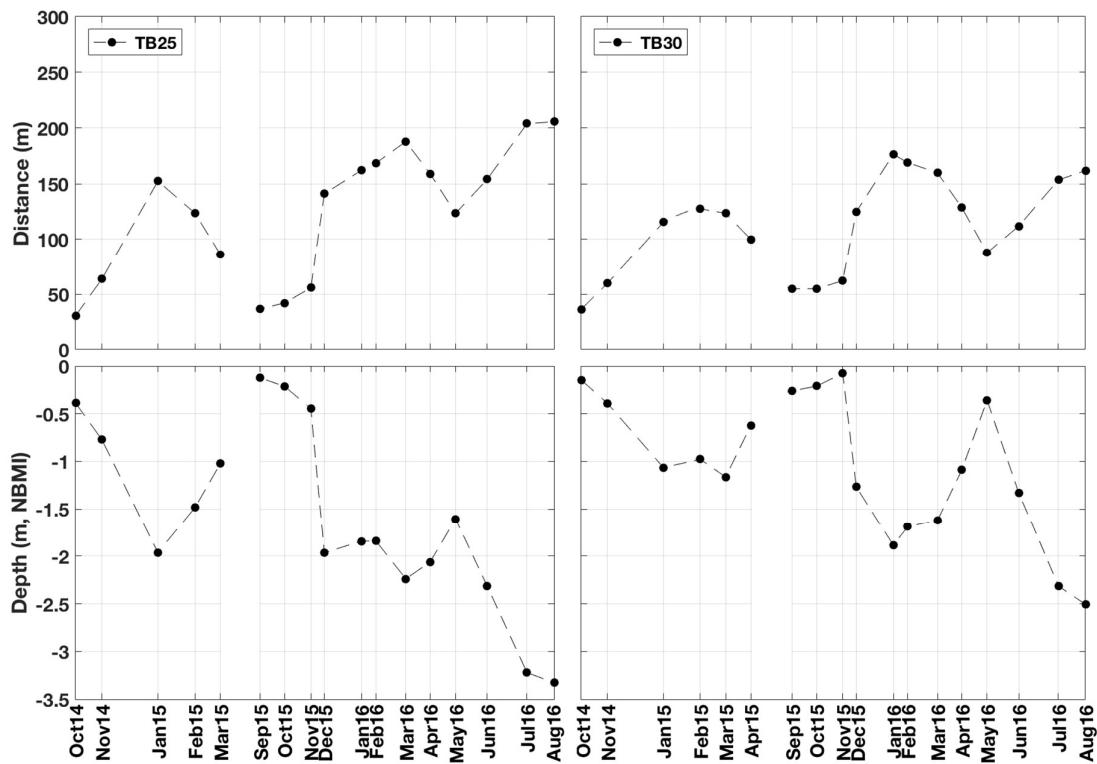


Figure 11. Cross-shore sandbar crest migrations (top panels) at TB25 and TB30 (northern beach) and their associated depths (bottom panels) from October 2014 to August 2016.

Periods of accretion and erosion are generally associated to low and high-energy wave conditions but they also exhibit strong site-specific variations (Sénéchal et al., 2015). In Ensenada beach the sandbars followed a cyclic morphological behavior, associated to periods of high and low wave energy (Ojeda et al., 2011; Ruessink et al., 2003). In contrast to studies in multi-barred beaches (Lippmann et al., 1993; Ruessink and Kroon, 1994; Shand et al., 1999; Plant et al., 1999), this single-barred beach presented a very strong seasonal response. The seasonal morphological variability and sandbar migration cycle of Ensenada beach for 2014 and 2015 coincides with the model proposed by Shepard (1950). In addition, the seasonal morphological changes agree with the suggested by Aagaard et al., (2013) and Sénéchal et al., (2015) for intermediate beaches.

The capability of the subaerial beach to fully recover from the winter erosion was attributed to the onshore sandbar migration during the summer mild wave conditions, which did not occur during the energetic 2015–2016 El Niño winter. In the winters before El Niño, the sandbar migrated offshore reaching 2 m depth from October to February. After February, it moved onshore during the post-winter milder waves welding the beachface by June, and incorporating the eroded sediment back onto the subaerial beach. During the 2015–2016 winter, however, the sandbar moved further offshore to deeper waters and the winter waves lasted for a month or two longer (till April 2016). The lack of long enough fair wave conditions from March to May is considered to be the cause of the inability of the sandbar to migrate onshore and weld the shoreline by June 2016.

## 6. Conclusions

Based on monthly measured bathymetric surveys from August 2014 to August 2016, this study investigated the cross-shore sandbar migration on the single-barred beach of Ensenada, Baja California. The sandbar formed near the shoreline by October 2014, and built up and moved offshore during the 2014–2015 winter from November to February, as a result of the subaerial beach erosion. During that winter the sandbar crest migrated 150–200 m offshore reaching an average depth of 2–2.5 m. The sandbar moved onshore after February 2015, merging the inner intertidal beach by May, and the sandbar and berm coexisted from March to April. The beach was unbarred during the 2015 summer waves from June to September, and a berm was built along the upper intertidal beach. The sandbar formed again by October 2015 and migrated 190–250 m offshore during the 2015–2016 El Niño winter, reaching depths of 3–3.5 m. Despite the onshore movement of the sandbar from February to April 2016, it was unable of welding the intertidal beach, thus, the beach was barred from June to August 2016. This study highlights the presence of a strong seasonal sandbar migration cycle in Ensenada Beach, which was interrupted during the 2015–2016 El Niño winter. The lack of long enough fair wave conditions in April and May 2016 is considered to be the cause of the inability of the sandbar to migrate onshore and weld the shoreline by June as it happened in 2014 and 2015.

## Acknowledgements

The authors are grateful to CONACyT for the funding provided through CB-2014-238765 and INFR-2013-011005 with the projects 205020 and 205022. Thanks are extended to F-PROMEP-38/Rev-03 SEP-23-005 and UABC for the support with UABC-PTC-418 and 18th project 636 (IMTENS). We are very thankful to all field assistants, especially to Eduardo Gil, Julio Lopez and Ernesto Carsolio for the technical support provided in the field, and to Angélica Romero for her support on some of the data processing.

## References

- Aagaard, T., Greenwood, B. and Hughes, M.G., 2013. Sediment transport on dissipative, intermediate and reflective beaches. *Earth-Science Reviews*, 124: 32–50.
- Adams, P.N., Inman, D.L. and Graham, N.E., 2008. Southern California deep-water wave climate: characterization and application to coastal processes. *Journal of Coastal Research*, 24:1022–1035.
- Allan, J.C., Komar, P.D., 2002. Extreme storms on the Pacific Northwest Coast during the 1997–98 El Niño and 1998–99 La Niña. *Journal of Coastal Research* 18 (1): 175–193.
- Coco, G., Sénéchal, N., Rejas, A., Bryan, K.R., Capo, S., Paristo, J.P., Brown, J.A., MacMahan, J.H.M., 2014. Beach responses to a sequence of extreme storms. *Geomorphology* 204:493–501.
- Di Leonardo, D. and Ruggiero, P., 2015. Regional scale sandbar variability: Observations from the U.S. Pacific Northwest, *Continental Shelf Research*, 95: 74–88.
- Grunnet, N.M. and Hoekstra, P., 2004. Alongshore variability of the multiple barred coast of Terschelling, The Netherlands. *Marine Geology*, 203: 23–41, ISSN 0025-3227.
- Blossier, B., Bryan, K.R., Daly, C.J., Winter, C., 2016. Nearshore sandbar rotation at single-barred embayed beaches, *Journal of Geophysical Research*, 121(4), 2286–2313.
- Henderson, S.M., Allen, J.S., Newberger, P.A., 2004. Nearshore sandbar migration predicted by an eddy-diffusive boundary layer model, *Journal of Geophysical Research*, 109, C06024.
- Hoefel, F. and Elgar, S., 2003. Wave-induced sediment transport and sandbar migration, *Science*, 299: 1885–1887.
- Lippmann, T.C., Holman, R.A., Hathaway, K.K., 1993. Episodic, Nonstationary Behavior of a Double Bar System at Duck, North Carolina, U.S.A., 1986–1991, *Journal of Coastal Research* SI 15: 49–75.
- Ojeda, E., Guillén, J., Ribas, F., 2011. Dynamics of single-barred embayed beaches. *Marine Geology*, 280: 76–90.
- Pape, L., Y. Kuriyama, y B.G. Ruessink, 2010. Models and scales for cross-shore sandbar migration, *Journal of Geophysical Research*, 115.
- Plant, N.G., Freilich, M.H., Holman, R.A., 2001. Role of morphologic feedback in surf zone sandbar response. *Journal of Geophysical Research*, 106: 973–989.
- Plant, N.C., Holman, R.A., Freilich, M.H., Birkemeier W.A., 1999. A simple model for interannual sandbar behavior, *Journal of Geophysical Research* 104: 15755–15776.
- Ruessink, B.G. and Ranasinghe R., 2014. *Beaches*. In: Masselink, G., and Gehrels R. (ed.), *Coastal Environments & Global Change*. American Geophysical Union: Wiley. Hardcover, 7: 149–176.

- Ruessink, B.G., Kuriyama, Y., Reniers, A.J.H.M., Roelvink, J.A., Walstra, D.J.R., 2007. Modeling cross-shore sandbar behavior on the timescale of weeks. *Journal of Geophysical Research*, 112, F0310.
- Ruessink, B.G., Wijnberg, K.M., Holman, R.A., Kuriyama, Y. and van Enckevort, I. M. J., 2003. Intersite comparison of interannual nearshore bar behavior. *Journal of Geophysical Research*, 108: C8 3249.
- Ruessink, B.G., Kroon, A., 1994. The behaviour of a multiple bar system in the nearshore zone of Terschelling: 1965–1993. *Marine Geology* 121, 187–197.
- Ruggiero P., Kaminsky G.M., Gelfenbaum G. and Cohn N., 2016. Morphodynamics of prograding beaches: A synthesis of seasonal- to century-scale observations of the Columbia River littoral cell. *Marine Geology*, 376: 51–68.
- Ruggiero P., Walstra D.J.R., Gelfenbaum G., 2009. Seasonal-scale nearshore morphological evolution: field observations and numerical modeling. *Coast Eng.*, 56: 1153–1172.
- Ruiz de Alegria-Arzaburu, A., García-Nava, H., Gil-Silva, E., Desplán-Salinas, G., 2015. A morphodynamic comparison of walled and non-walled beach sections, Ensenada beach, Mexico. World Scientific. *The Proceedings of the Coastal Sediments* ISBN: 978-981-4355-52-0. Shand et al., 1999
- Sénéchal, N., Coco G., Castelle B. and Marieu V., 2015. Storm impact on the seasonal shoreline dynamics of a meso- to macrotidal open sandy beach (Biscarrosse, France), *Geomorphology*, 228: 448–461.
- Storlazzi, C., Griggs, G., 2000. Influence of El Nino-Southern Oscillation (ENSO) events on the evolution of central California's shoreline. *Geological Society American Bulletin* 111, 236–249.
- Van de Lageweg, W.I., Bryan, K.R., Coco, G., Ruessink, B.G., 2013. Observations of shoreline-sandbar coupling on an embayed beach. *Marine Geology*, 344, 101–114.
- Walstra, D.J.R., 2016. On the anatomy of nearshore sandbars: A systematic exposition of inter-annual sandbar dynamics (*Doctoral thesis*, Delft University of Technology).
- Wijnberg, K.M., and Terwindt, J.H.J., 1995. Extracting decadal morphological behavior from high-resolution long-term bathymetric surveys along the Holland coast using eigenfunction analysis. *Marine Geology* 126, 301–330.
- Yuhi, M., Matsuyama, M., Hayakawa, K., 2016. Sandbar Migration and Shoreline Change on the Chirihama Coast, Japan. *Journal of Marine Science and Engineering*, 4:40.